A COMPARISON OF INTERACTIONAL AERODYNAMICS METHODS FOR A HELICOPTER IN LOW SPEED FLIGHT

John D. Berry
US Army, ATCOM, AFDD
Hampton, VA, USA

Victor Letnikov and **Irena Bavykina**
Mil Moscow Helicopter Plant
Moscow, Russia

Mark S. Chaffin
Lockheed Martin
Hampton, VA, USA

Abstract

Recent advances in computing subsonic flow have been applied to helicopter configurations with various degrees of success. This paper is a comparison of two specific methods applied to a particularly challenging regime of helicopter flight, very low speeds, where the interaction of the rotor wake and the fuselage are most significant. Comparisons are made between different methods of predicting the interactional aerodynamics associated with a simple generic helicopter configuration. These comparisons are made using fuselage pressure data from a Mach-scaled powered model helicopter with a rotor diameter of approximately 3 meters. The data shown are for an advance ratio of 0.05 with a thrust coefficient of 0.0066. The results of this comparison show that in this type of complex flow both analytical techniques have regions where they are more accurate in matching the experimental data.

Introduction

Rotorcraft configurations have always presented a challenge to the accurate prediction of vehicle aerodynamic performance. Complex lifting surfaces operating in a characteristically unsteady environment present challenge enough, but coupling this flow with the shapes common to helicopter fuselages amplifies the complexity. Often the prediction of isolated rotor aerodynamics is coupled using superposition with linear aerodynamic fuselage analyses or measured isolated fuselage data. Previous studies (reference 1 and 2) of complete helicopter configurations have shown weaknesses in the linear superposition assumptions commonly used in the design cycle. However, accurate models for the complex aerodynamic interactions between the rotor and the fuselage have not been developed as general tools available to the helicopter designer.

Non-linear interaction effects arise in the aerodynamics of helicopter configurations in several cases. Among these cases clearly the wake of the rotor affects the fuselage onset flow. The wake geometry in most inflow models is assumed to be undisturbed by the fuselage. The wake does distort due to the presence of the fuselage. This distortion increases as the wake skew angle decreases (at lower speeds where the wake washes over the body). The influence of the fuselage on the inflow to the rotor is also potentially significant. The additional inflow distortion to the presence of the fuselage produces a change in the aerodynamics of the blades. This effect changes the strength of the shed wake and contributes to additional distortion of the wake.

Notation

Ct Thrust Coefficient, thrust/(density x disk area x tip speed x tip speed)

Cp Pressure Coefficient, (pressure - freestream pressure)/freestream dynamic pressure

R Radius of the rotor, 1.574 m (62 in.)

X Downstream length, m (in)

Y Lateral distance, m (in)

Z Vertical length, m (in)

A1s Longitudinal Flapping angle, degrees

Experimental Data

The Langley 14- by 22-Foot Subsonic Tunnel

The Langley 14- by 22-Foot Subsonic Tunnel is a closed-circuit, single-return, atmospheric wind tunnel (figure 1). In 1970 the unusual test requirements associated with V/STOL and rotorcraft aerodynamic research led to design and construction of this tunnel. The tunnel has a test

section that can be operated in a variety of configurations: closed, slotted, partially open, and open. The closed test section is 14.5 ft high by 21.75 ft wide by 50 ft long with a maximum speed of about 338 feet per second (fps). The open test section configuration, which has a maximum speed of about 270 fps, is formed by raising the ceiling and walls to form a floor-only configuration. The tunnel may be configured with a moving-belt ground plane and a floor boundary-layer removal system at the entrance to the test section for ground-effects testing. During this investigation the tunnel was configured with the walls and ceiling in the raised position to improve the quality of the low speed flow.

Figure 1: Langley 14- by 22-Foot Subsonic Tunnel

The tunnel is equipped with an on-line static data reduction system that can display computed aerodynamic coefficients with interactions and wall interference corrections in real time. The tunnel has support, drive, and instrumentation to facilitate powered rotorcraft testing and has been used for rotorcraft investigations since its inception. In addition, the tunnel has flow-visualization and acoustic testing capabilities.

Rotor Test System

The rotor test system used for the experimental data reported here is built on a generic test system developed at the 14- by 22-Foot Subsonic Tunnel. This test system, the General Rotor Model System (GRMS), consists of two synchronous electric motors, a combining gearbox, collective and cyclic blade pitch controls and a four-bladed articulated hub mounted on a six-component strain-gauge balance. It also includes a fuselage skin mounted on a separate, similar balance. These two six-component strain-gauge balances are used to provide independent measurement of the rotor and fuselage aerodynamic loads. The system as tested is shown in figure 2 installed in the wind tunnel.

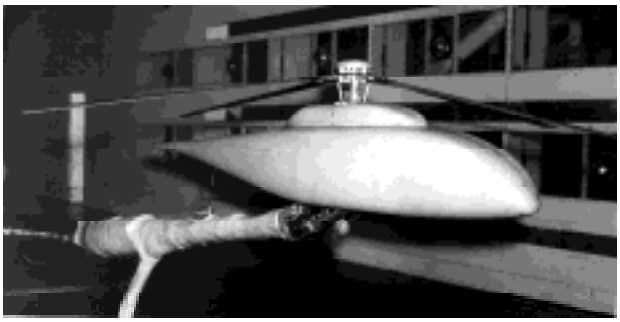

Figure 2: GRMS and Fuselage in Langley 14- by 22-Foot Subsonic Tunnel

The rotor system tested consisted of four rectangular blades on an articulated hub. The blades have a linear twist of -8.0 degrees from the center of rotation to the tip. The chord of 4.25 inches and radius of 62.0 inches gives the system a solidity of 0.087.

The shape of the fuselage is designed to be representative of a wide range of helicopter fuselages without being specific to any one. The fuselage can be described by a set of super-ellipse equations that simplifies development of computer models. The geometry of this fuselage is described in references 2 and 3 and is shown in figure 3.

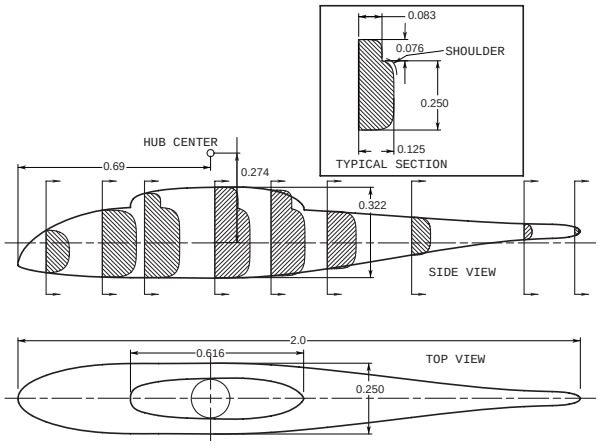

Figure 3: ROtor Body INteraction (ROBIN) Fuselage (units of rotor radius)

Test Procedure

The pressure measurements were made at several flight conditions (reference 3). Although these conditions ranged in lift, forward speed, and propulsive task this comparison will be limited to a single representative low-speed condition. The advance ratio for this representative condition was 0.05. A non-dimensional thrust coefficient of 0.00659 was set with a shaft angle of -2.0 degrees relative to the free-stream. The rotor tip speed was 648.9 feet per second. The rotor cyclic controls were trimmed to reduce once-per-

revolution flapping of the rotor blades with respect to the rotor shaft to -0.81 degrees of longitudinal flapping and 0.07 degrees of lateral flapping.

Pressure measurements were made using an array of scanning pressure transducers. Pressure taps were arranged in strips of taps at constant X stations. Only the average pressure values could be obtained with the instrumentation available during this investigation. The helicopter model is mounted on a sting support system that fits to the bottom of the fuselage and trails the model. In the region of attachment to the fuselage the sting attachment affects the pressure values that were measured.

Computational Methods

Two methods of computing the interaction of the helicopter rotor and its wake with the fuselage will be shown in this work. The first method is based on techniques that model the flows associated with the helicopter. This method has been developed by Mil using models developed for the analysis of helicopter flows (reference 4). The second method shown is based on the solution of the Navier-Stokes equations for the main flow. The effect of the main rotor in this method is approximated using a pressure jump boundary condition at the rotor disk. This method has been developed by the Aeroflightdynamics Directorate (AFDD) of the US Army (reference 5).

Mil Method

This work presents some results of the study of flow over a helicopter fuselage at the low horizontal velocity condition with the influence of the main rotor. In these calculations allowances were made for wake contraction and for variability of convection velocity of free vortices. An assumption was made that the free vortices were moving down with a velocity averaged over azimuth. However this average velocity varies with blade radius and according to the vertical distance from the rotation plane of the rotor. Other details of this method are described in reference 4.

The method shown here is computed in sequence on personal-computer class of work stations. As such, this method could be incorporated in a comprehensive helicopter analysis to be a computationally efficient method for simulation of the aerodynamic influence of a rotor-fuselage configuration. Six main sub-programs are used in this method.

1. The main starting and linking program.

2. A program to provide the geometrical breakdown of the fuselage surface and a wake in the case of flow separation at the fuselage aft.

3. A program for the approximation of the wake shape when separating at the fuselage aft using the method described in reference 6.

4. A program for calculating the flow over the fuselage.

5. A program to determine the velocities induced by the fuselage and its wake at any point in space.

6. A program to calculate the streamlines on the fuselage surface.

The fuselage geometry is broken down into panels using an automated procedure. The resulting panels for the Mil calculation are shown in figure 4 along with the experimental transducer stations. Interpolation is required between the computed surface pressures at the panel centers to the locations of the measured pressures.

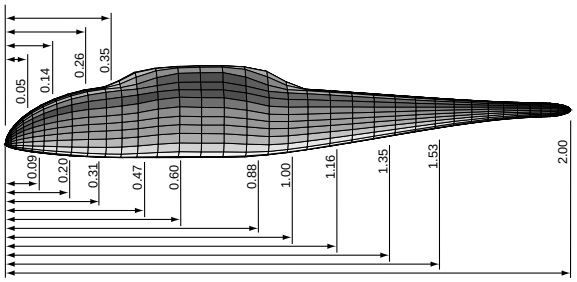

Figure 4: Panels Used for Mil Fuselage Model

First, an isolated rotor was considered to choose values of collective pitch and longitudinal deviation of the swashplate that produce the necessary thrust coefficient Ct and the flapping angle A1s. Then the velocity induced by the rotor on the fuselage was calculated and pressure distribution was defined.

The calculations of the flow over the fuselage were carried out in the velocity field induced by the rotor and averaged over time. To determine the time-averaged influence of the main rotor, the entire rotor wake was computed at three azimuths with an interval of 30 degrees. Since there are four blades in this rotor system, this average is equivalent to a full rotation.

At the next stage the effect of the fuselage upon the rotor was defined. The collective pitch at the rotor and the longitudinal deviation of the swashplate were slightly corrected, and the pressure distribution over the fuselage was redefined. It is not necessary to continue the iterative process due to the small influence of the fuselage upon the rotor at the given condition; then the calculation was stopped.

AFDD Method

The choice of a Navier-Stokes code for this work was made to insure that regions of fuselage that would naturally separate could be predicted without a priori knowledge of the geometry of this separation. An incompressible Navier-Stokes code (reference 7) is the basis for the method used in this study since the relative speeds seen by the fuselage are incompressible. The use of a Navier-Stokes code for rotorcraft application requires either a detailed grid system that describes the rotor system and relative motion of the rotor blades or a model for the lifting rotor. For the work described here, the rotor system was modeled by a pressure discontinuity at the rotor disk. The compressible effects of the rotor blade are accounted for using the blade element theory and tabular values for the lift and drag of the airfoil at each rotor section.

The pressure discontinuity at the rotor disk was computed iteratively with the solution to the flowfield. This pressure value was computed using blade element theory and the current values of the flowfield at each location on the rotor disk. This computation also included blade pitch trim to attain the desired rotor net force and direction.

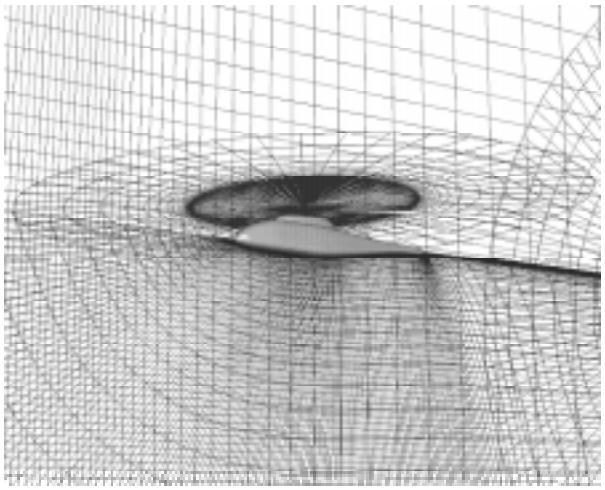

Figure 5: AFDD Grid for ROBIN and Rotor

The grid system that was used for the calculation of the helicopter flowfield consists of several overset grids. Interpolation of the flowfield properties in the overlapping regions of the grids was used as the boundary condition for the inner grids. A global outer grid was used to prescribe the actual flow condition to the code. The overlapping inner grids are shown in figure 5.

The relative cost of doing a complete Navier-Stokes simulation of helicopter configurations at low speed is high. Over 60 Cray C-90 hours were required for this case.

Results and Discussion

The character of the aerodynamics at low speeds can be seen in the flow solution obtained using the AFDD method. Figure 6 shows computed flow at the flight condition studied. Since the AFDD model uses steady flow, streamlines (shown in sub-figure 6(a)) can be computed to show the general directions taken by the flow. Shading on the fuselage in sub-figure (a) indicates changes in surface pressure. The stagnation of the rotor wake over the nose of the fuselage is clearly shown in this figure. In subfigure 6(b) the concentration of vorticity in the flow is shown by means of the lateral (Y) component of vorticity. This figure shows the effective envelope of the rotor wake and the influence of the fuselage on this shape. The wake skew angle computed by momentum for this condition is approximately 45 degrees. From the figure, the leading edge of the wake envelope is approximately 50 degrees with respect to the rotor disk normal. The trailing edge of the wake envelope (although clearly not fully developed) is less than the leading edge, approximately 42 degrees. Beyond the solution region examined, the net wake skew angle appears to be consistent with that predicted by momentum.

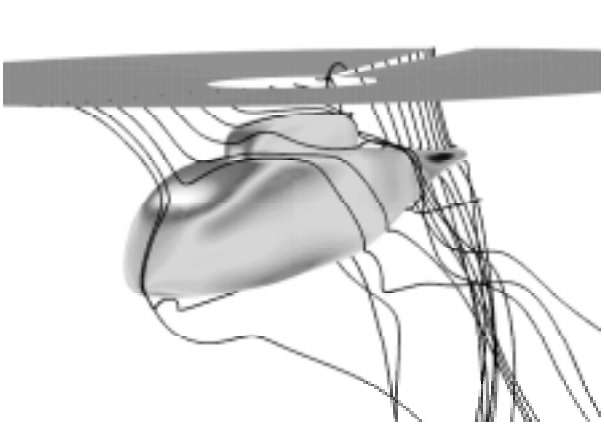

(a) Streamlines Released from the Disk Centerline

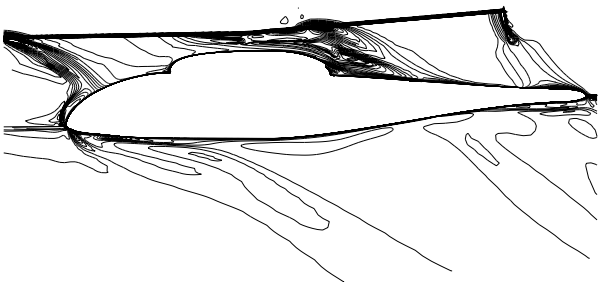

(b) *Y* Vorticity Contours

Figure 6: Flow Computed from the AFDD Solution

Comparisons of the computed and experimental pressures are shown in the following figures. Each figure compares the two prediction methods

with the experimental data at one downstream (X/R) station. The results are plotted as pressure coefficients (on an inverted scale) as a function of vertical location (Z/R) on the body. For reference the vertical location of the rotor hub is Z/R = 0.274.

At the extreme nose of the fuselage (figure 7) the AFDD solution matches the experimental pressures well. The Mil solution may suffer from the coarse panel spacing and the interpolation to the measurement location.

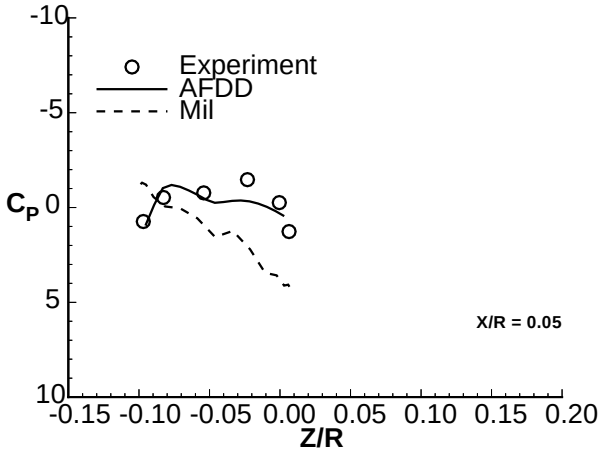

Figure 7: Pressure Comparison at X/R=0.05

At the second X/R station (figure 8) a better match is seen between the two computational methods than in figure 7. Both methods show less suction over the "shoulder" of the model than seen in the experiment. The shoulder is the region of the cross-section (shown in figure 3) where the radius of curvature is the smallest. However, the Mil method does not capture the shoulder acceleration at all. This may still be due to the coarse panel spacing that does not match the curvature of the geometry in this region.

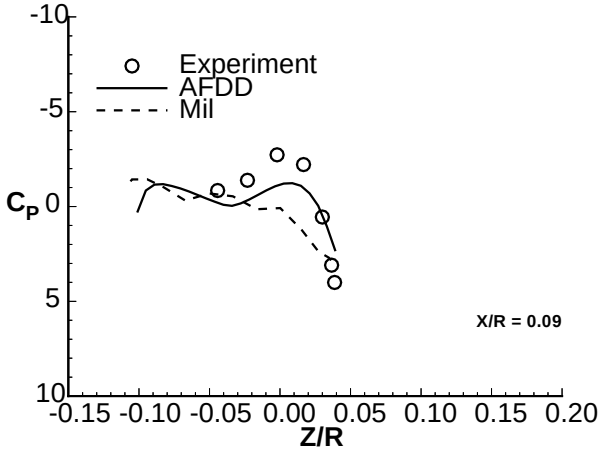

Figure 8: Pressure Comparison at X/R=0.09

The trend of both computational methods to underpredict the suction at the shoulders of the configuration continues at stations up to that measured at X/R = 0.31 (figures 8 to 12).

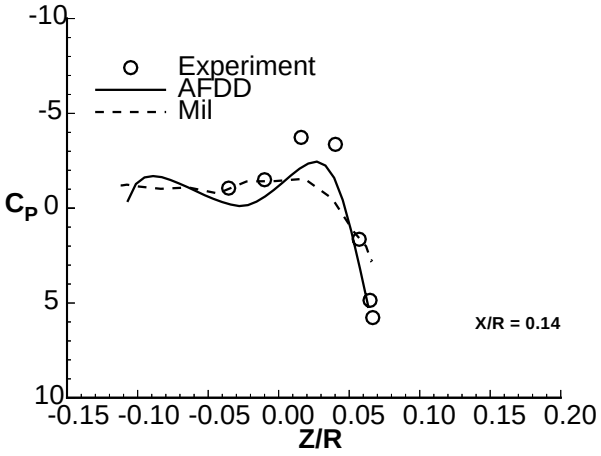

Figure 9: Pressure Comparison at X/R=0.14

At more downstream locations on the nose (from X/R= 0.14 - 0.35) the Mil method improves in predicting the shoulder suction. At X/R = 0.14 (figure 9) hardly any suction is predicted by the Mil method while the AFDD solution shows a clear "peak" in the suction similar in trend to the experimental data.

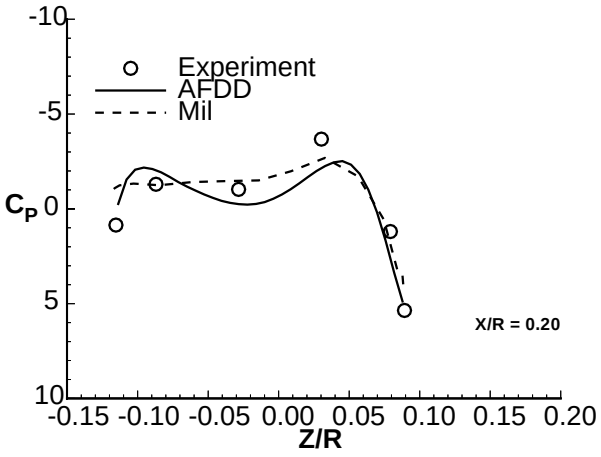

Figure 10: Pressure Comparison at X/R=0.20

At X/R = 0.20 (figure 10) both methods show a "peak" in the suction over the shoulder of the section. At this station both methods agree well with the experiment, except at the bottom of the fuselage where the data indicate a deceleration of the flow. This deceleration is over-predicted by the AFDD method.

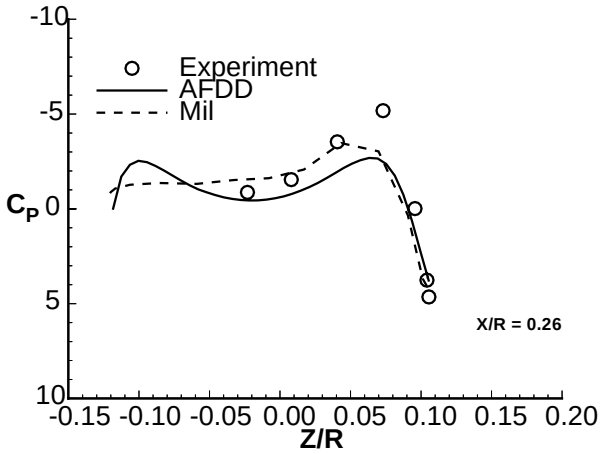

Figure 11: Pressure Comparison at X/R=0.26

The data from the nose section at X/R = 0.26 (figure 11) indicates that the flow experiences approximately twice the suction at the shoulder than predicted by either method.

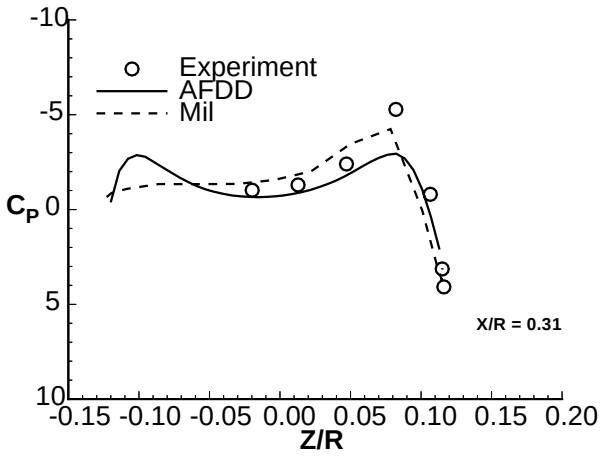

Figure 12: Pressure Comparison at X/R=0.31

In figure 12 the shoulder suction is matched better by the Mil method than by the AFDD method, although this may result from the close spacing with specific wake filaments at a specific azimuth of wake used to produce the Mil average influence.

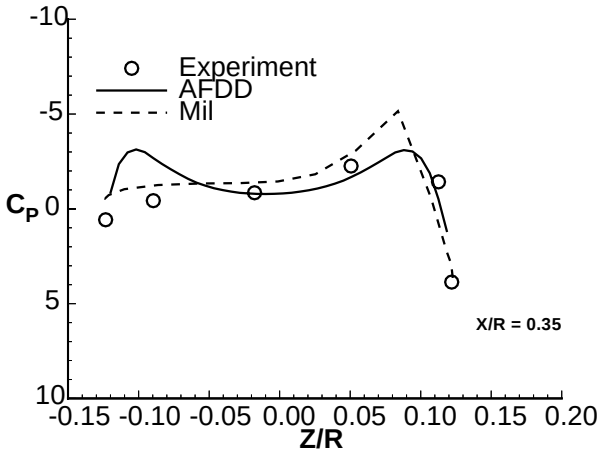

Figure 13: Pressure Comparison at X/R=0.35

At the section at X/R = 0.35 (just before the nacelle region of the fuselage) both the Mil and AFDD methods predict a shoulder suction peak between measured data points. At this section the AFDD method continues to predict a deceleration around the bottom of the section. The data at this section indicate a separation, not a deceleration at the bottom of the section. In fact, at this section the Mil prediction follows the trend of the experimental data better than the AFDD method at the bottom. The implication here is that the Navier-Stokes model does not accurately predict the separation that is apparent in the data.

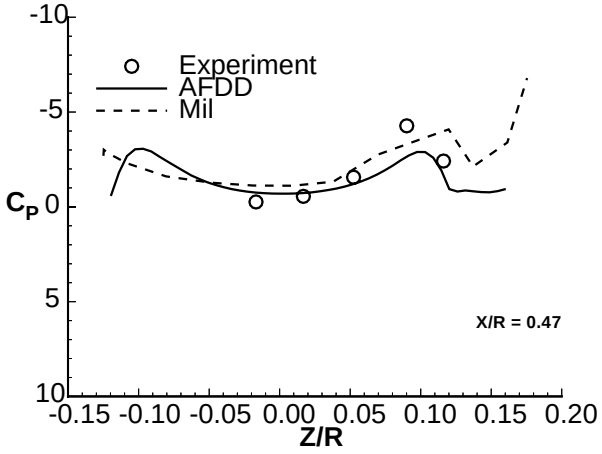

Figure 14: Pressure Comparison at X/R=0.47

Although no pressure data were obtained on the nacelle region of the fuselage, it is clear that the two methods disagree in the character of the surface pressures over the nacelle at the section X/R = 0.47. The prediction of shoulder peak suction in the Mil solution for this section suffers from coarse panel interpolation, since the precise geometry of the nacelle-body junction is lost.

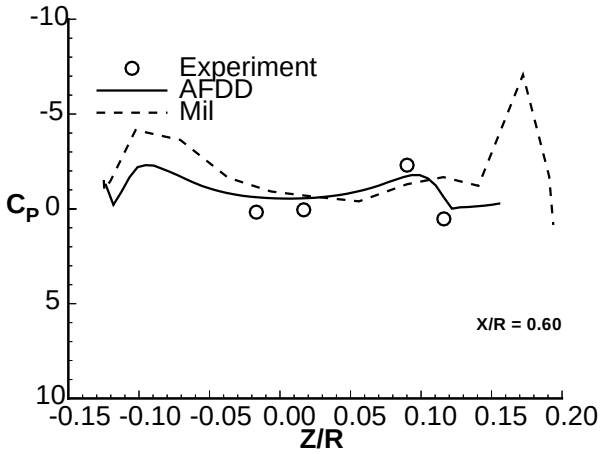

Figure 15: Pressure Comparison at X/R=0.60

At the X/R = 0.60 section only four experimental data points are available for correlation. The AFDD solution best fits all four of these points, while the Mil solution is a good fit to the lower three. Again, similar to the prediction at X/R = 0.47, the two methods are in significant disagreement on the character of the flow on the nacelle of the fuselage.

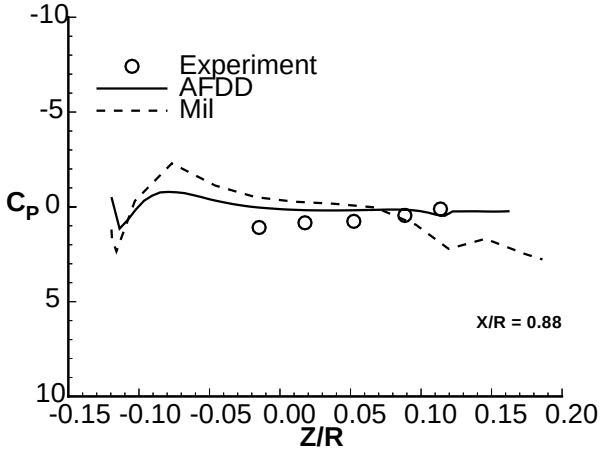

Figure 16: Pressure Comparison at X/R=0.88

Although both predictive methods show that the flow at X/R = 0.88 is relatively benign, there is a discrepancy with the experimental data. The data at this station are most affected by the influence of the model support. The contribution of the support is not included in either solution method.

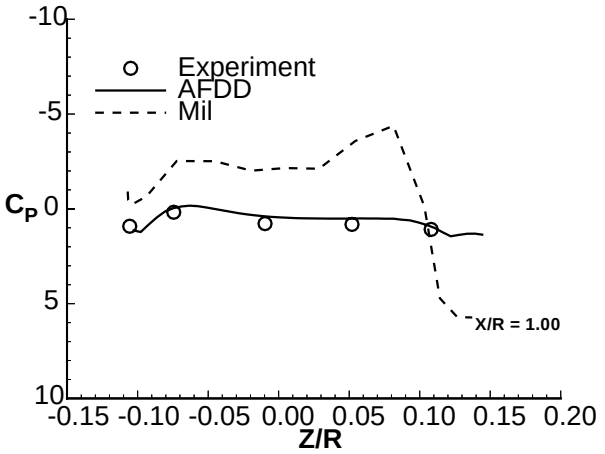

Figure 17: Pressure Comparison at X/R=1.00

At locations behind the rotor (X/R > .8) the Navier-Stokes method predicts very small and relatively uniform values of surface pressures. In this region, the Mil method predicts an accelerated flow with the lowest pressures on the fuselage where there are relatively sharp edges that will force flow acceleration. Specifically at section X/R = 1.00, the AFDD prediction shows, with surprising accuracy, the influence of the fuselage separation seen in the experimental data while the Mil method shows a stagnation behind the nacelle (approximately Z/R of 0.14) and a strong acceleration over the shoulder (approximately Z/R of 0.09).

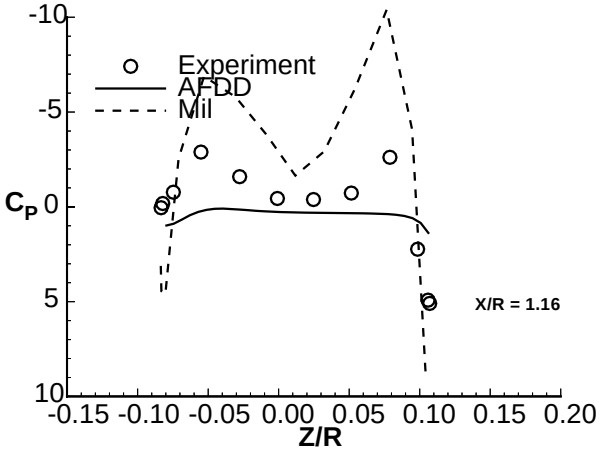

Figure 18: Pressure Comparison at X/R=1.16

Behind the nacelle, the influence of the accelerated rotor wake on the surface pressures is demonstrated by the Mil method and seen in the experimental pressures. Although the magnitudes are not predicted accurately, the trend of the Mil prediction is good. This overprediction in the magnitude of the surface suction may be due to the influence of the filaments that are used to model the rotor wake and their close influence on the panel solution. The AFDD method, in contrast, completely misses the acceleration of

the flow on the shoulder and bottom edge of this section. This is, perhaps, due to the numerical diffusion of the velocity gradients in the inner sheets of the rotor wake by this time-averaged numerical method. This diffusion may cause an overprediction of the region of separation.

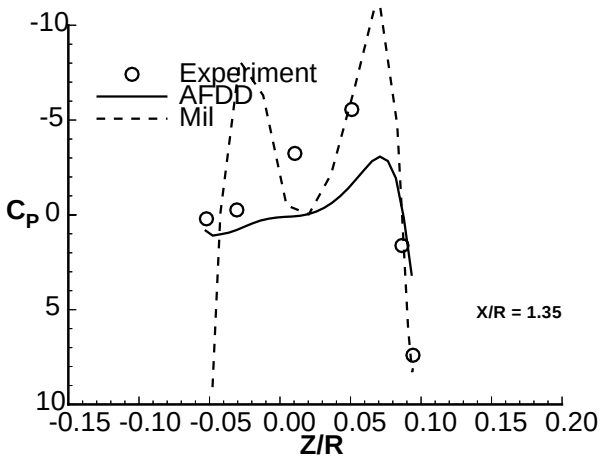

Figure 19: Pressure Comparison at X/R=1.35

Mid-way down the tail region (X/R = 1.35) the Mil method continues to show the strong interaction between the wake and the fuselage pressures at the top and bottom corners of the fuselage. In this region the fuselage transitions from the super-ellipse shape with well-defined corners to a round section. The experimental data show the influence of the wake as an acceleration (or suction) over the shoulder. The bottom of the fuselage, however, returns to a base pressure indicating separation. Here the AFDD method, although not accurate in magnitude, matches the trend of the experimental pressure.

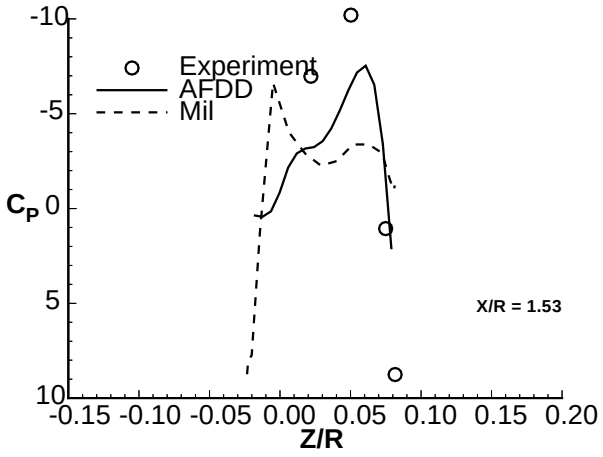

Figure 20: Pressure Comparison at X/R=1.53

At the final station where experimental data are available, X/R = 1.53, only four experimental pressure ports are available. Similar to the mid-tail station (figure 19) the AFDD prediction seems to capture the trend of the experimental data. At the middle of this section both predictive methods have a similar magnitude that is well below that of the experimental data. This indicates that the mean velocity of the flow at this station is underpredicted.

Concluding Remarks

A comparison of methods for the prediction of fuselage aerodynamics at low speeds has been made with one set of experimental data. In general, both methods provide insight into this complex flow with good general agreement with the experimental pressure distribution. From this limited comparison, some specific observations can be made:

- The total cost of producing an engineering estimate for a rotor-fuselage combination is much lower for the model-based approach of Mil when compared with the Navier-Stokes approach of the AFDD methodology.

- Although the AFDD method correctly predicts the influence of separation behind the nacelle region, the apparent separation below the fuselage ahead of the nacelle is not captured well by this Navier-Stokes method.

- The choice of breaking the fuselage into a specific number of panels will result in some inaccuracies in the representation of the air flow. This inaccuracy shows itself in the comparison of the flow on the extreme nose of the fuselage.

- Over the nacelle, where there is no experimental data, the two predictive methods show significantly differing flow characteristics.

- Just aft of the nacelle the acceleration of the flow by the wake is seen in the Mil prediction of the fuselage pressure, but missed by the AFDD method that shows only a region of separation.

References

1. Sheridan, P. F. and Smith, P. R.: "Interactional Aerodynamics – A New Challenge to Helicopter Technology," in proceedings of the 35th Annual Forum of the American Helicopter Society, Washington, D. C., May 1979, pp 79-59-1–79-59-15.

2. Berry, J. D. and Althoff, S. L., "Inflow Velocity Perturbations Due to Fuselage Effects in the Presence of a Fully Interactive Wake," In proceedings of the 46th Annual Forum of the American Helicopter Society, Washington, D. C., May 1990, pp 1111–1120.

3. Freeman, C. E. and Mineck, R. E.: “Fuselage Surface Pressure Measurements of a Helicopter Wind-Tunnel Model with a 3.15-Meter Diameter Single Rotor,” NASA TM 80051, March 1979.

4. Letnikov, V. B. and Bavykina, I. D.: “Calculation of the Aerodynamic Interaction Between Rotor, Wing and Fuselage” Mil Moscow Helicopter Plant Report No. 880/5-USA, December 1995.

5. Chaffin, M. S. and Berry, J. D.: “Helicopter Fuselage Aerodynamics Under a Rotor by Navier-Stokes Simulation” *Journal of the American Helicopter Society*, **42**:3, July 1997.

6. Poltz, G. and Quentin, J., “Separated Flow Around Helicopter Bodies,” in proceedings of the 7th European Rotorcraft and Powered Lift Aircraft Forum, 1981.

7. Rogers, S. E., Kwak, D., Kiris, C.: "Steady and Unsteady Solutions of the Incompressible Navier-Stokes Equations," *AIAA Journal*, Volume 29, Number 4, April 1991, pp. 603–610.

Appendix — Mil Fuselage Panelization

Calculation of an attached flow around a fuselage is an important part of the general design of the fuselage. For this purpose a method based on a theory of potential flows is used. A solution is sought as a potential of velocity perturbations. A distribution of the potential over the fuselage surface is presented as a sum of potentials of a double layer and a single one.

The fuselage is broken down into a finite number of panels and a no penetration boundary condition {of opacity} is applied in the center of every panel. It is assumed that distribution of the double layer and the single {simple} one are constant over each of the panels. The density of the double layer is determined using a given external field of velocities. In calculating the surface integrals an assumption is used that the panels of the fuselage breakdown are right-angled. Changing from the real fuselage to the right-angled panels causes {any} distortions at corners of the rectangles. However these distortions have little influence on the results since the no penetration conditions {of opacity} are enforced at centers of the panels. This is especially true as the number of the panels increases since these inaccuracies will grow smaller. As a result, a system of equations in unknown potentials of the double layer was solved on each of the panels. The solution was sought by an iterative method.

The fuselage breakdown into the panels is a key element directly preceding the calculation. The breakdown into the panels has to render the fuselage shape as exactly as possible on one hand and on the other hand to be convenient for calculation of velocities on its surface via an unknown distribution of the potential.

The fuselage breakdown into panels has direct influence both on the convergence of the iterative process and on the accuracy of the results obtained. Programs were developed for the fuselage breakdown and for control over the obtained panels. These programs locate the panel centers, calculate the lengths and directions of the normals and tangents to the surface, and enable a visual inspection {of the validity of their assignment} using graphical displays.

We assign a system of coordinates X, Y, Z to the fuselage with the X axis as longitudinal. The fuselage is intersected with the some planes normal to the X axis. Positions of these planes are selected based on accordance with specifics of the fuselage geometry. The lines of Intersection of these planes with the fuselage surface create up closed contours.

A relative center may be chosen for each of these contours (a center of mass of the cross-section may be taken assuming mass to be constant over the surface). The contours are divided into an equal number of parts. Then each of the real contours are projected onto a unit circle with its center at the center of mass, equal angles onto the real contour of the section, and each unit circle is divided into subintervals equal in angle. Associated points on the real contour can be taken as reference points. In cases of the complicated contours, an irregular breakdown with unequal angles should be used.

As a result, each of the cross-sections will be divided in an angle into an equal number of the parts. The fuselage breakdown into the panels can be realized by joining the proper points of the adjacent contours. The panels constructed in this way are generally not flat. The angles formed by their sides are not right. So, additional operations are carried out to form each of the panels. The resulting panel geometry is shown in figure 4.

As a result, radius vectors of the panel centers in the adopted system of coordinates, unit normal vectors, unit vectors of one of the tangents (located in a longitudinal section of the fuselage), and lengths of two mutually perpendicular directions are computed for each of the panels.

The complexity of the fuselage shape results in a disorganized arrangement of the panel centers where the potential is to be determined. This disorganized arrangement presents difficulties for computing the velocities tangent to the surface by differentiation of the potential.

It is convenient to use the fuselage breakdown already at our disposal to avoid a double approximation of the potential over the whole surface. Calculating total velocity at a given point requires only derivatives of the potential with respect to length in two different directions. We can use the given tangent vector of the tangent located in the fuselage longitudinal plane as one of the directions. A vector located in the plane perpendicular to the X axis and tangent to the fuselage contour in the given section is conveniently used as the second direction. To determine the direction of this tangent, the contour at the given point is approximated with a circle.